(Received 18 May 2024, Accepted 18 July 2024, Scheduled 8 August 2024)

Design of a Compact Dual Port 2×1 Ultra-Wideband MIMO Antenna for Radio Frequency Energy Harvesting Based on Four ``A" Shaped Slots

Amira A. Khedr*, Basem E. Elnaghi, and Ahmed M. Mohamed

Electrical Engineering Department, Faculty of Engineering, Suez Canal University, Ismailia 11566, Egypt

ABSTRACT: Radio frequency energy harvesting (RF-EH), which uses an ultra-wideband (UWB) antenna, is the best substitute for traditional batteries for continuously powering sensor networks. The UWB antenna helps to receive the ambient radio frequency energy that radiates from communication applications for harvesting purposes to power devices or recharge batteries. A novel aspect of this design is the use of dual antenna ports with four "A" shaped slots in radiating patches and ground plane, which permits the harvester to completely utilize all accessible frequency bands. The design analysis of a compact dual-port (2×1) ultra-wideband multiple-input multiple-output (UWB-MIMO) antenna based on four "A" shaped slots and shared ground plane in the band of 2.3–21.7 GHz is presented. The proposed antenna has been implemented on a Rogers RT 5880 substrate with a size of 39 mm $\times$ 30 mm, a thickness of 0.8 mm, and a dielectric constant of 2.2. It achieves $S_{11} \leq -10$ dB at (2.3–21.7) GHz and a maximum peak gain of 10.29 dB at 20.53 GHz. The proposed antenna is designed and simulated with ANSYS HFSS and fabricated. The results of simulation and measurement of the proposed antenna are in good agreement, and the antenna achieves bandwidth of 2.3–20 GHz that supports radio frequency energy harvesting in addition to UWB applications across satellite, Wi-Fi, Wi-Max, and mobile applications.

1. INTRODUCTION

With the rapid development of the Internet of Things (IoT), which meets human needs in various fields such as work, study, and entertainment, sensors have become more ubiquitous and are interconnected to form Wireless Sensor Networks (WSNs), which require continuous power to keep it running [1–4]. Batteries, which are frequently used as a traditional power source in low-power electronic devices such as sensors, require periodic and routine maintenance in the form of recharging or replacement, which is expensive and impractical, especially when the sensors are in hard-to-reach places [5].

Consequently, the energy harvesting (EH) technology is a candidate solution that aims to recharge batteries by harvesting energy from ambient environmental sources, such as solar, wind, and Radio Frequency (RF) energy. Therefore, if the energy source is continuously available, such as RF energy, which is present in daily devices including radio towers, Wi-Fi routers, cell phones, satellites, and communication applications, the sensors can be operated continuously [6, 7].

An RF energy harvesting system consists of a rectifying antenna (Rectenna) that receives ambient RF energy through a receiving antenna and converts the harvested energy into usable direct current (DC) through a rectification circuit to provide energy, especially for low-power applications [8].

RF energy can be captured using various types of antennas, such as wide-band (WB) and ultra-wideband (UWB) antennas. UWB antenna is attracting interest owing to its wider bandwidth. The Federal Communications Commission (FCC) assigned a frequency range for UWB technology, which extends between 3.1 GHz and 10.6 GHz [9]. UWB antenna designs are classified into two types: planar and non-planar. However, planar UWB antennas have received more attention in research because of their low profile, lower cost of manufacture, and multiple types of design, such as: printed monopole [10], tapered aperture [11], metamaterial structure [12], and microstrip UWB antenna [13]. Microstrip patch antenna has attracted more attention from the researcher because of its many advantages, including its low cost, small size, lightweight nature, and ease of fabrication. Microstrip antenna is composed mainly of four parts: radiating patch, dielectric substrate, ground plane, and feed line [14].

Several planar UWB antenna design mechanisms have been studied, such as a single UWB antenna element of different lengths and shapes, and these single antennas have either limited antenna gain, increased design complexity, or inefficiency in producing DC [15, 16]. Also, the material of the antenna substrate has a significant impact on antenna performance parameters and efficiency. Even though FR4 is a common substrate material used in patch antenna designs [17], it suffers from performance limitations at higher frequencies due to dielectric losses, making it unsuitable for many RF applications. In contrast, Rogers has excellent high frequency performance and low signal loss, making it an ideal choice for harvesting electromagnetic energy [18, 19]. Furthermore, applying different-sized and shaped slots to the ground plane and radiator patch is the simplest method to construct a planar UWB

* Corresponding author: Amira Ali Khedr (amira.ali.pgs@eng.suez.edu.eg).

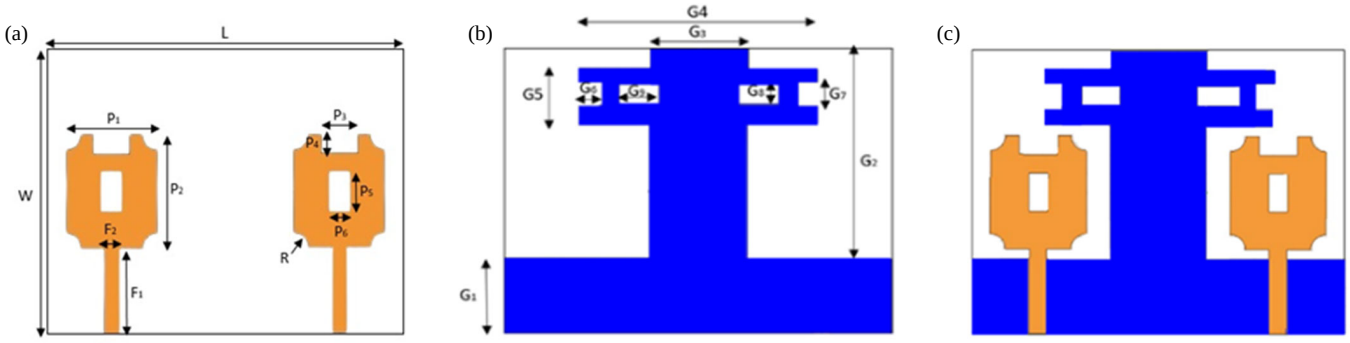

FIGURE 1. Proposed antenna: (a) radiating patches, (b) ground plane and (c) final model.

antenna [20–22]. Additionally, the receiving UWB antenna is connected to the rectifying circuit. The amount of energy captured by the receiving antenna and the rectifier circuit's conversion efficiency are the main factors affecting the system's overall performance, and a high gain antenna enhances harvesting power [23–25]. While ambient power levels are low, the harvested energy should be increased. This may be accomplished in two main ways. First, the rectifying circuit's efficiency should be maximized to the highest acceptable level. Second, multiple diversity techniques can be used to improve the overall power received by the rectenna [26].

However, RF energy in the ambient environment has a low power density. Therefore, it is difficult for a single antenna to capture significant energy from a certain frequency range, reducing the received RF energy and system efficiency [27]. To address this, multi-antenna technology with multiple-input multiple-output (MIMO) antennas has been designed to increase the harvested RF power due to multiport [28, 29], and improve higher gain [30, 31], resulting in a high RF-to-DC conversion efficiency. Since the design of MIMO antennas consists of more than one element, coupling between the ports is an important issue in MIMO design, which reduces the performance of the MIMO antenna [32].

The isolation between the ports in MIMO antennas plays an important role in energy harvesting. High isolation enables each antenna to independently capture RF energy from a variety of sources. This results in a more efficient energy harvesting system capable of receiving and converting RF energy from a wide range of sources [33]. Thus, to improve the isolation between the ports, several decoupling methodologies have been adopted such as: using a metamaterial-based MIMO antenna [34–36], octagonal shaped MIMO antenna [37], and Split Ring Resonator (SRR) antenna [38] to get excellent isolation. Also, the MIMO antenna with an orthogonal construction offers better isolation between the ports [39, 40].

Furthermore, the performance of a MIMO antenna system is characterized by several critical diversity parameters, including Envelope Correlation Coefficient (ECC), which evaluates the correlation between the antenna elements; Diversity Gain (DG), which quantifies the improvement in signal quality received through the multiple antennas; Mean Effective Gain (MEG), which measures the average gain in a specific direction; and Total Active Reflection Coefficient (TARC), which evaluates the reflections and losses within the antenna system [41, 42].

While the MIMO antenna used in energy harvesting systems acts as a receiver and does not transmit signals, it can still provide significant benefits to the system in terms of improved gain, diversity performance, and efficiency, thereby maximizing harvested energy [43, 44].

Therefore, the utilization of UWB MIMO antennas is a candidate technology used in EH systems because of its distinctive features, which allow the harvester to increase captured RF energy in the surrounding environment [45]. However, based on our research, most of the publications on UWB-MIMO antennas have had some shortcomings in the design, such as large size, certain operating frequency band, mainly the 2.4 GHz band, and complex decoupling completely use each of the accessible frequency bands for structures.

Hence, this paper presents the design analysis of a dual-port (2×1) UWB-MIMO antenna based on four "A" shaped slots and shared ground plane, with a compact size of 39 mm $\times$ 30 mm, a thickness of 0.8 mm, and simple decoupling structures via a strip feed line that enables the harvester to capture the ambient radio frequency in the bands between 2.3 and 21.7 GHz. This paper is organized as follows. Section 2 describes the proposed antenna design steps and analysis Radio Frequency Energy Harvesting (RFEH) purposes. Section 3 contains thorough examinations of the simulated and measured parameters, as well as the reflection coefficient, surface current distribution, radiation pattern characteristics, gain, radiation efficiency, and diversity performance. Finally, Section 4 shows the conclusion.

2. FORMULATION

2.1. Antenna Design and Analysis

The proposed compact dual-port (2×1) UWB-MIMO antenna structure is fabricated on a Rogers RT 5880 substrate with dimensions of 39 mm $\times$ 30 mm $\times$ 0.8 mm, a loss tangent of 0.0009, and a dielectric constant of 2.2 as shown in Figure 1.

This structure has four "A" shaped slots, two in radiating patches fed by a strip line as presented in Figure 1(a), and the other two in the shared ground plane to broaden bandwidth as presented in Figure 1(b). ANSYS HFSS was used to optimize antenna parameters. Table 1 lists the dimensions of the final proposed antenna model shown in Figure 1(c).

TABLE 1. Optimized values of the proposed antenna in (mm).

Parameters	L	W	P_1	P_2	P_3	P_4	P_5	P_6	F_1	F_2
Values	39	30	10	12	4	2	4	2	9	1.8
Parameters	R	G_1	G_2	G_3	G_4	G_5	G_6	G_7	G_8	G_9
Values	0.0016	10	24	6	4	2	22	2.5	2	8

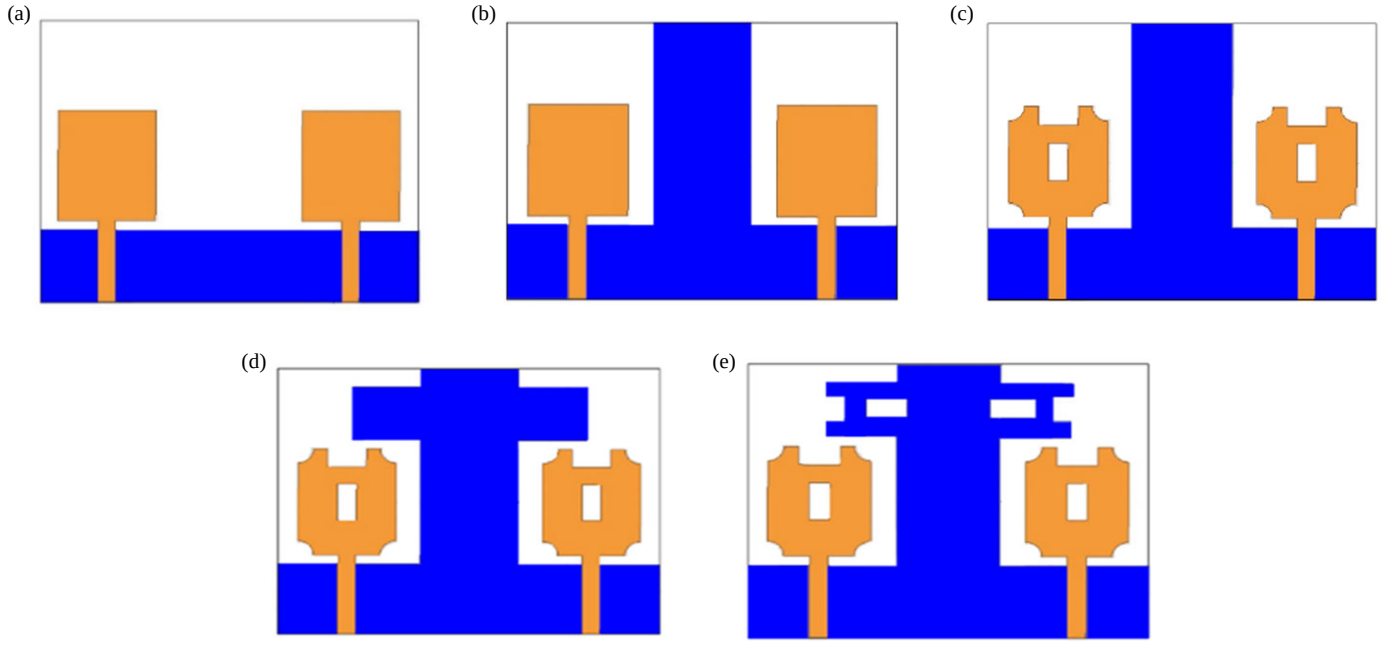

FIGURE 2. Design steps of the proposed antenna: (a) step 1, (b) step 2, (c) step 3, (d) step 4, (e) step 5.

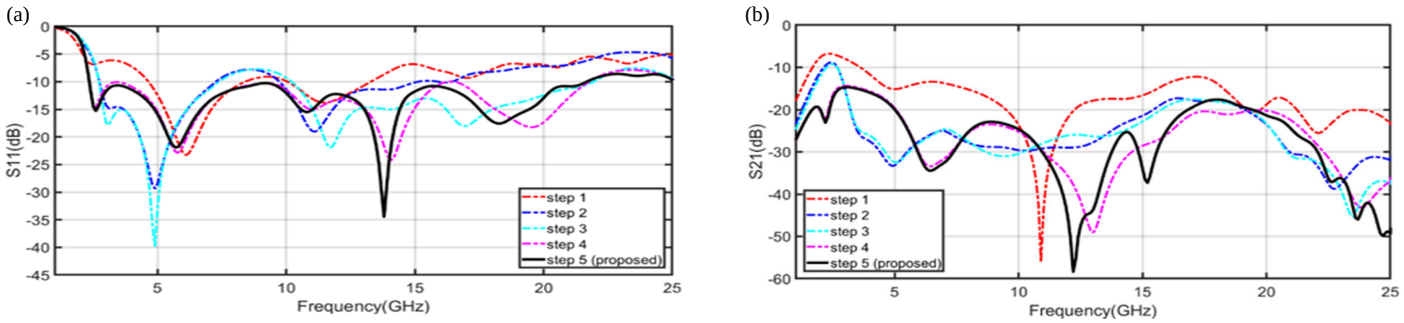

FIGURE 3. Simulated S-parameters (a) S_{11}, (b) S_{21} curves of the antenna design steps.

2.2. Design Steps

Five steps were implemented to obtain the proposed antenna design for energy harvesting purposes, as shown in Figure 2. Additionally, Figures 3(a) and (b) present the impact of the antenna design steps on their reflection coefficients (S_{11}) and mutual coupling coefficients (S_{21}), respectively. The first step of the design is shown in Figure 2(a), which has two radiating patches and a common rectangular ground plane. The antenna in step 1 has a reflection coefficient from 4.6 GHz to 13.3 GHz, although between 8.4 GHz and 10 GHz, there is a portion of $S_{11} \geq 10$ dB as shown in Figure 3(a). The next step is step 2 as presented in Figure 2(b), which includes adding a vertical rectangular strip to the common ground plane to increase the impedance bandwidth. As a result, the reflection coefficient is now (2.7–15) GHz, but we still need to get rid of a portion of the band that is greater than -10 dB at (7.2–9.6) GHz.

To address this, we etched the four corners in each radiating patch and inserted two reverse "A" shaped slots slots on it, as seen in Figure 2(c), which is step 3. Thus, to meet the needs of ultra-wideband applications, this step increases the bandwidth

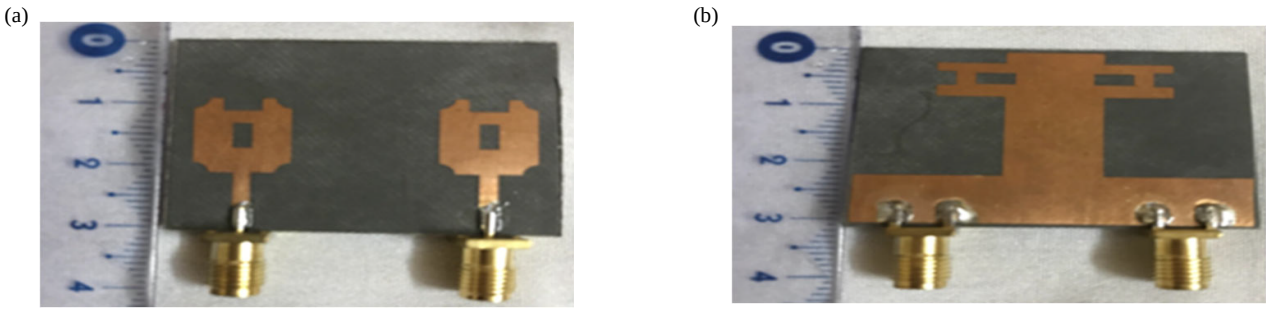

FIGURE 4. (a) Top view and (b) bottom view of the fabricated proposed antenna.

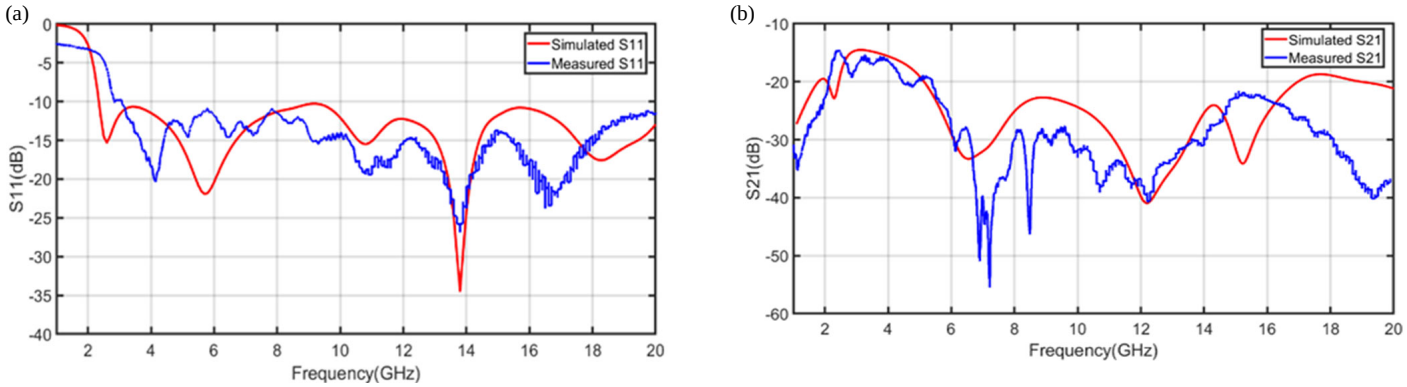

FIGURE 5. (a) Reflection coefficient and (b) mutual coupling coefficient comparison between simulated and measured.

to be from 2.7 GHz to 22 GHz. Another horizontal rectangular strip is added to the shared ground plane in step 4, as presented in Figure 2(d), to increase the impedance bandwidth to be from 2.3 GHz to 22 GHz. However, the bands at 9 GHz and 16 GHz touch -10 dB, so we attempt to fade away this by inserting two "A" shaped slots to the last rectangular strip added in step 4 to the shared ground plane to be the final step as shown in Figure 2(e), which is step 5. Moreover, step 5 (the proposed antenna) operational frequency range can cover the required UWB to be (2.3–21.7) GHz as seen in Figure 3(a) and achieve better isolation between ports than the previous steps as presented in Figure 3(b), making it suitable for the radio frequency energy harvesting applications.

3. RESULTS ANALYSIS

To test the performance of the proposed antenna, prototype hardware has been fabricated. Figures 4(a) and (b) show the top and bottom views of the prototype antenna. The proposed UWB MIMO antenna performance is examined via scattering parameters, surface current distribution, radiation pattern, gain, radiation efficiency, and diversity performance.

3.1. Scattering Parameters

Figures 5(a) and (b) compare the reflection coefficient and mutual coupling coefficient of the proposed MIMO antenna between simulated and measured ones, respectively. There is a good match between the simulated and measured performances, with a little shift in frequency caused by cable losses and manufacturing mistakes. The S-parameters of the proposed MIMO antenna are measured by using a Vector Network Analyzer (VNA) as shown in Figure 6. The MIMO antenna's measured and simulated reflection coefficients (S_{11}) are less than -10 dB from 2.8 GHz to 20 GHz in measured terms and from 2.3 GHz to 21.7 GHz in simulated terms as seen in Figure 5(a), with fractional bandwidth of 150.8% and 161.6% in measured and simulated terms, respectively. The proposed antenna has maximum return losses of -20.2 dB (measured) and -22.56 dB (simulated) at 5.8 GHz resonance frequency, as well as -26.3 dB (measured) and -34.7 dB (simulated) at 13.8 GHz

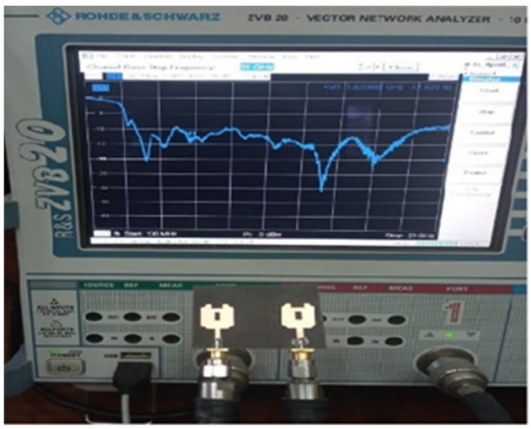

FIGURE 6. The VNA's MIMO antenna testing procedure.

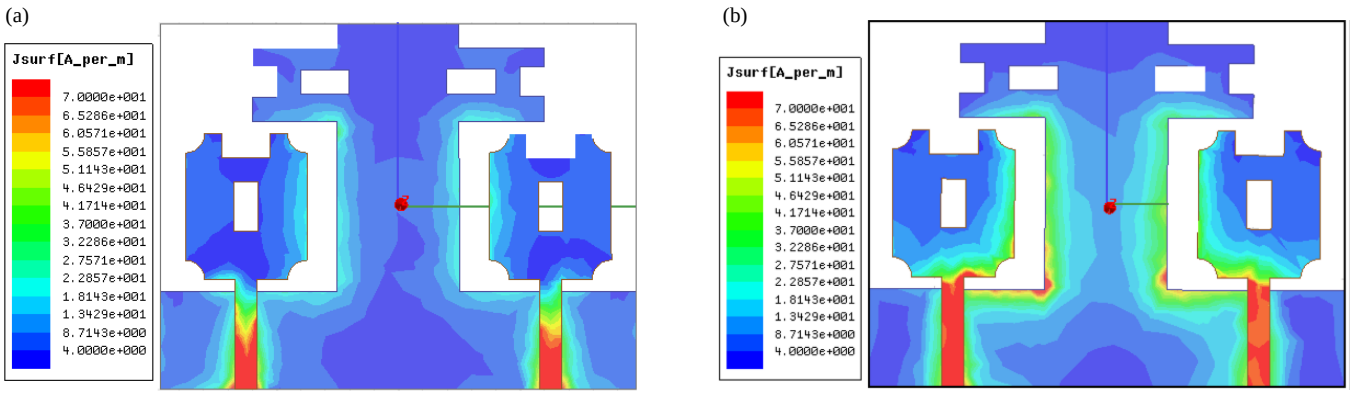

FIGURE 7. Surface current distribution of the proposed antenna in different frequencies. (a) 2.4 GHz, (b) 5.8 GHz.

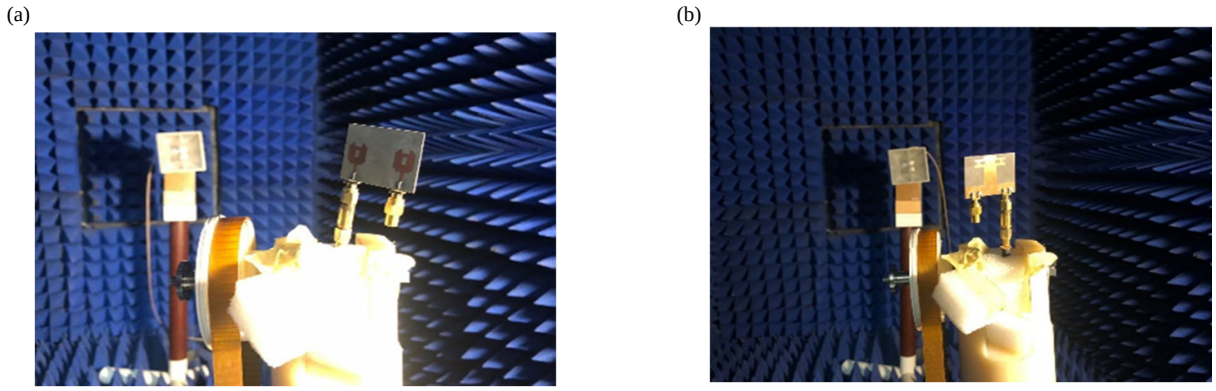

FIGURE 8. Photograph of the (a) top view and (b) bottom view of the proposed antenna in anechoic chamber.

resonance frequency. Significant improvements in isolation between the proposed antenna's ports have been made, and throughout the operating band, mutual coupling coefficient levels greater than (16.31 dB with a 60 dB peak value in measured) and (19.91 dB with a 40.91 dB peak value in simulation) are observed as shown in Figure 5(b). According to the measured and simulated scattering parameters and mutual coupling coefficient results, the proposed MIMO antenna exhibits acceptable impedance matching over the spectrum of possible RF bands in the surrounding environment.

3.2. Surface Current Distribution

The current distributions on the radiating patch's surface and ground plane's surface have a significant impact on the antenna sensitivity, according to the antenna performance theory. Due to the feed line's connection to the feed point (excitation port), which results in a higher concentration of current there than in other areas of the antenna, it is evident that the highest current amplitude occurs at this location [46].

Figure 7 illustrates the surface current distribution at frequencies of 2.4 GHz presented in Figure 7(a) and 5.8 GHz presented in Figure 7(b). According to the graph, the surfaces of the radiating patch and ground plane exhibit a modest current, which progressively decreases away from the feed line. This demonstrates that the antenna's design may effectively and sensitively capture electromagnetic waves.

3.3. Radiation Pattern

The proposed MIMO antenna's radiation characteristics are measured in an anechoic chamber, as shown in Figure 8. An anechoic chamber is a quiet region with no losses due to no reflection inside the room [47]. Because of its symmetrical design, radiation parameters are only examined at one port, and it is assumed that the other port displays the same behavior. The 2D far-field radiation simulation and measurement patterns shown in Figure 9 are a result of studying the proposed MIMO antenna's radiation performance at 5.8 GHz. There is good agreement between simulation and measurement. To maximize RF energy harvesting in the system, the antenna should be capable of receiving maximum RF energy from many frequencies in all directions of the environment [48]. According to the graph, the proposed MIMO antenna receives the most radiation in all directions in the E-plane as seen in Figure 9(a) and generates a quasi-omnidirectional pattern in the H-plane as seen in Figure 9(b). This indicates that the proposed antenna has the ability to receive signals from almost all directions, which is useful in environments where RF energy sources are distributed and not concentrated in one direction.

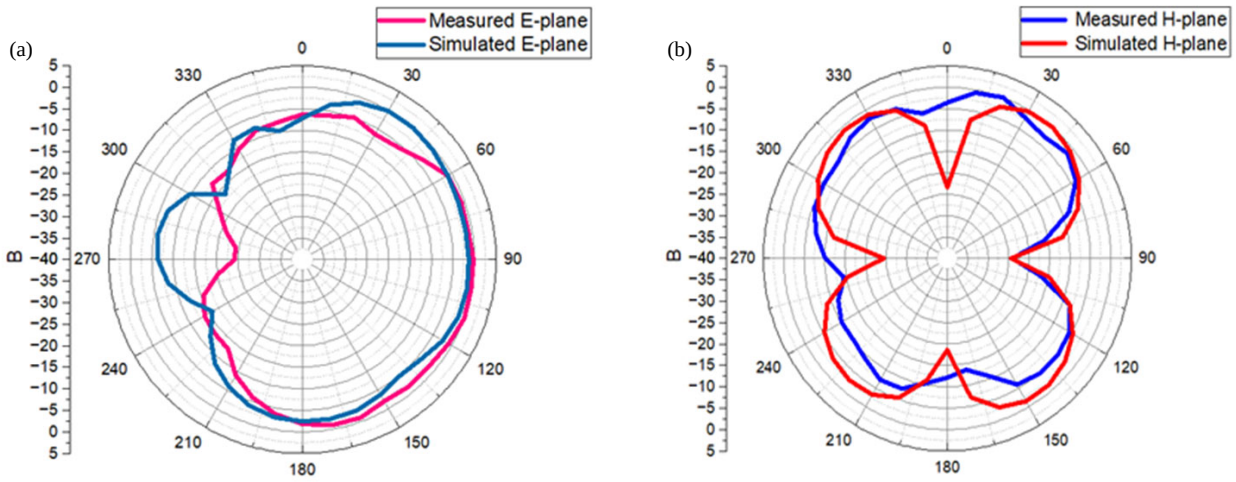

FIGURE 9. Measured and simulated radiation pattern at 5.8 GHz in (a) E-plane and (b) H-plane.

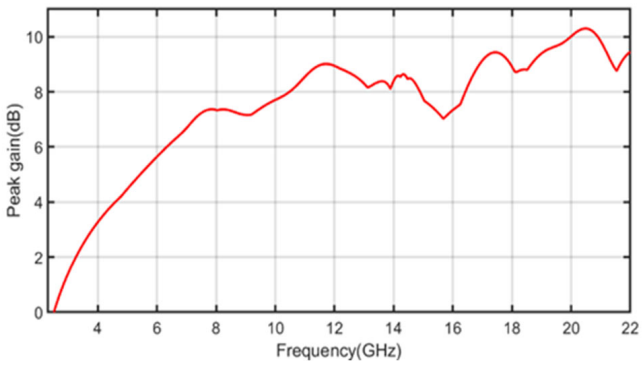

FIGURE 10. Antenna peak gain of the MIMO.

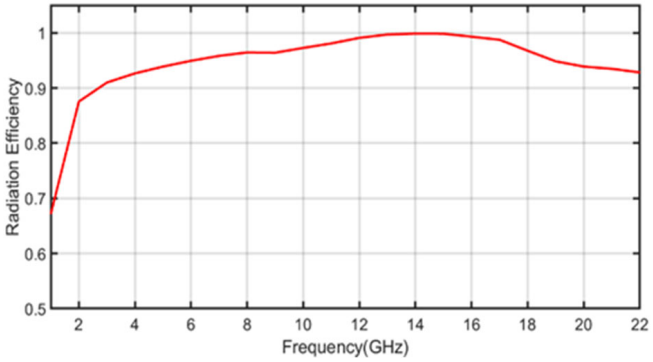

FIGURE 11. Antenna radiation efficiency of the MIMO antenna.

3.4. Antenna Gain and Efficiency

The simulated gain of the MIMO antenna is shown in Figure 10. The antenna has a moderate gain of 5.42 dB at 5.8 GHz and swings significantly around 9 dB throughout the operational band, with a maximum value of 10.29 dB at 20.53 GHz.

Figure 11 displays the proposed MIMO antenna radiation efficiency versus the operating frequency. It is obvious that the radiation efficiency of the antenna achieves 89% at the lower operating frequency of 2.3 GHz and increases across the whole operating band to achieve 93% at 21.7 GHz, with a maximum value of 99% at 13.5 GHz.

Hence, the gain of the proposed antenna increases gradually as the frequency increases. Therefore, the antenna provides omnidirectional or quasi-omnidirectional radiation at the lower frequencies, as shown in Figure 12, which presents the 3D radiation pattern at 5.8 GHz, while at the higher frequencies it tends to provide high-gain directive radiation. Overall, with the high efficiency of the antenna, it demonstrates good performance in terms of the gain across the intended band.

The power density and levels of RF signals in the environment are low [49]. An antenna design must have high gain and radiation efficiency in order to capture sufficient power, where high gain focuses the received energy more effectively, and high radiation efficiency ensures reduced losses in the antenna system. Then, the high proposed antenna gain and radiation efficiency are beneficial for capturing RF energy at very low RF power levels.

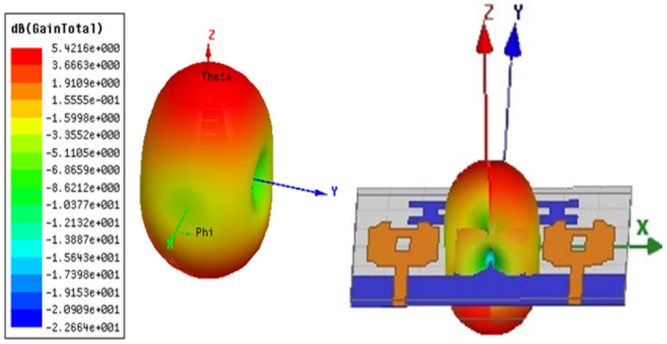

FIGURE 12. 3D radiation patterns at 5.8 GHz.

3.5. Diversity Performance

Multipaths in the environment may be considered, and antenna diversity is a solution for quasi-omnidirectional RF reception to increase the likelihood of receiving energy [50]. Therefore, diversity performance, which can be measured by metrics like the envelope correlation coefficient (ECC), diversity gain (DG), and total active reflection coefficient (TARC), plays a crucial

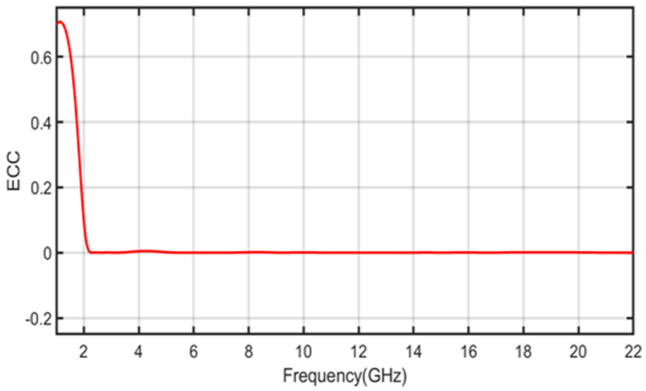

FIGURE 13. Simulated ECC for the proposed.

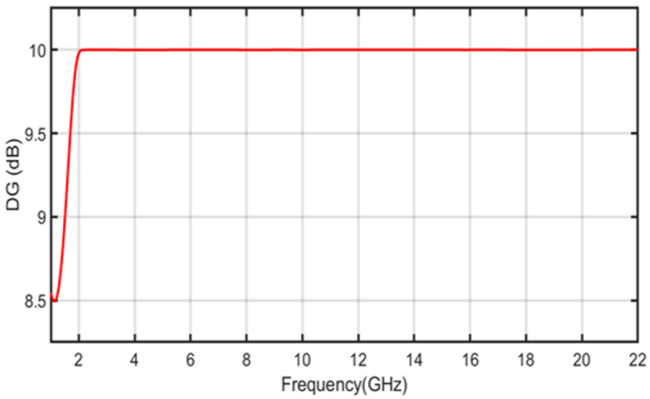

FIGURE 14. Simulated DG for the proposed antenna.

TABLE 2. Comparison of proposed antenna with published work.

Ref.	Size (mm^3)	BW (GHz)	Peak Gain (dBi)	Material	ECC	Eff. (%)
[12]	$20 \times 34 \times 1$	2.46–13.98	5.71	FR4	< 0.003	> 91
[33]	$44 \times 44 \times 1.6$	2.8–12	6.5	FR4	< 0.14	92
[41]	$71.7 \times 46.7 \times 1.6$	2.4	4.7	FR4	< 0.0035	95.2
[51]	$30 \times 30 \times 1.6$	3.1–12	6.2	FR4	< 0.001	87
[52]	$58 \times 58 \times 0.787$	4.4–14.4	5.3	Rogers RT 5880	< 0.01	90
[53]	$26 \times 31 \times 0.78$	2.8–12	5	Rogers RO 4003	< 0.001	> 95
[54]	$62.5 \times 60.5 \times 1.6$	3.5–11	4	FR4	< 0.01	70–90
This work	$39 \times 30 \times 0.8$	2.3–21.7	10.29	Rogers RT 5880	< 0.001	> 93

role in antenna performance for improving the efficiency of energy harvesting systems.

This section examines the diversity performance of the proposed MIMO antenna based on these three terms. For two radiating elements, ECC and DG are calculated using the formulae provided in [20] in terms of scattering characteristics, as shown directly in formulas (1) and (2).

$$\mathrm{ECC} = \frac{\left|S_{ii}^{*}S_{ij} + S_{jj}^{*}S_{ji}\right|^{2}}{\left(1-\left(|S_{ii}|^{2}+|S_{ji}|^{2}\right)\right)+\left(1-\left(|S_{jj}|^{2}+|S_{ij}|^{2}\right)\right)} \quad (1)$$

$$\mathrm{DG} = 10\sqrt{1-(\mathrm{ECC})^{2}} \quad (2)$$

The ECC was used to measure the isolation and correlation between the antenna elements. Lower ECC values indicate higher isolation and a lack of correlation between the devices. Thus, improve energy harvesting by ensuring that the energy received by each antenna element comes from a variety of uncorrelated sources, potentially improving the total harvested energy. Furthermore, diversity gain improves the system's ability to discover and exploit weak RF signals, which is critical for energy harvesting in situations where the RF power level is low. This guarantees that even low-level ambient RF energy is properly transformed into useful power.

The ECC and DG simulation results are shown in Figure 13 and Figure 14, respectively. We can see that ECC is close to zero across the impedance bandwidth, which indicates high isolation between the proposed antenna elements. However, DG was approximately 10 dB throughout the whole UWB range.

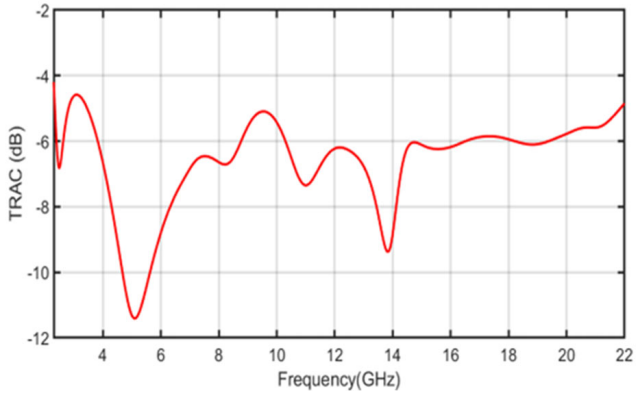

FIGURE 15. Simulated TARC for the proposed antenna.

The TARC is defined as the square root of the total reflected power and apparent return loss of the total incident power for the entire operating frequency of the MIMO antenna. For a dual-port MIMO antenna, TARC can be calculated according to the method proposed in [51], as shown in formula (3):

$$\mathrm{TARC} = \frac{\sqrt{\left(s_{11}+s_{12}\right)^{2}+\left(s_{21}+s_{22}\right)^{2}}}{\sqrt{2}} \quad (3)$$

Figure 15 shows the simulated TARC result. It is evident that the simulated TARC value is below 4.58 dB in the entire op-

erational frequency. Thus, the proposed UWB MIMO antenna has good diversity performance results, which is intended to support UWB applications and RF energy harvesting.

4. PERFORMANCE COMPARISON

Table 2 compares the performance of the proposed UWB MIMO antenna with that of other related studies. It is evident that the proposed antenna provides a wider bandwidth, better gain, high efficiency, and low ECC value. Additionally, it is easy to model and fabricate at low cost. In addition, the Rogers RT 5880 substrate used in the proposed antenna design provides a higher frequency band than FR4. Thus, the proposed UWB MIMO antenna can be efficiently used for energy harvesting purposes and UWB applications.

5. CONCLUSIONS

A dual-port (2×1) UWB MIMO antenna with four "A" shaped slots and common ground plane is presented. The proposed antenna was implemented on a 39 mm $\times$ 30 mm $\times$ 0.8 mm Rogers RT 5880 substrate. The designed antenna had an impedance bandwidth of 2.3 to 21.7 GHz and low mutual coupling less than -15 dB. The proposed antenna has a maximum gain value of 10.29 dB at 20.53 GHz with good diversity performance: ECC is approximately equal to zero, DG roughly 10 dB, and TRAC below 4.58 dB. The radiation efficiency of the proposed MIMO antenna is between 89% and 93% within the whole operating frequency, with a maximum efficiency of 99%. The proposed antenna is fabricated, and according to the simulated and measured results, the proposed antenna may be a good option for RF energy harvesting systems.

REFERENCES

[1] Li, X., S. Liu, S. Kumari, and C.-M. Chen, "PSAP-WSN: A provably secure authentication protocol for 5G-based wireless sensor networks," *Computer Modeling in Engineering & Sciences (CMES)*, Vol. 135, No. 1, 711, 2023.

[2] Chu, S.-C., T.-K. Dao, J.-S. Pan, and T.-T. Nguyen, "Identifying correctness data scheme for aggregating data in cluster heads of wireless sensor network based on naive Bayes classification," *EURASIP Journal on Wireless Communications and Networking*, Vol. 2020, 1–15, 2020.

[3] Fan, F., S.-C. Chu, J.-S. Pan, C. Lin, and H. Zhao, "An optimized machine learning technology scheme and its application in fault detection in wireless sensor networks," *Journal of Applied Statistics*, Vol. 50, No. 3, 592–609, 2023.

[4] Eltresy, N. A., A. E. M. A. Elhamid, D. M. Elsheakh, H. M. Elhennawy, and E. A. Abdallah, "Silver sandwiched ITO based transparent antenna array for RF energy harvesting in 5G mid-range of frequencies," *IEEE Access*, Vol. 9, 49 476–49 486, 2021.

[5] Williams, A. J., M. F. Torquato, I. M. Cameron, A. A. Fahmy, and J. Sienz, "Survey of energy harvesting technologies for wireless sensor networks," *IEEE Access*, Vol. 9, 77 493–77 510, 2021.

[6] Yakine, F. and A. Kenzi, "Energy harvesting in wireless communication: A survey," in *E3S Web of Conferences*, Vol. 336, 00074, 2022.

[7] Pavithra, B. G. and M. Arunadevi, "Review on RF energy harvesting," *International Journal of Engineering Research & Technology (IJERT)*, Vol. 5, No. 22, 2017.

[8] Elbendera, S. A., A. Allam, A. M. Mohamed, R. Pokharel, and A. B. Abdel-Rahman, "Design of an ultra-wideband antenna for ambient radio frequency energy harvesting in 10.88–33.66 GHz," in *2022 16th European Conference on Antennas and Propagation (EuCAP)*, 1–5, Madrid, Spain, 2022.

[9] Sarkar, A., S. Sultana, A. Paul, and M. M. Rashid, "Study on ultra-wideband (UWB) system and its applications," *J. of the Bangladesh Electronics Society*, Vol. 18, No. 1-3, 01–05, 2018.

[10] Muzaffar, S., D. Turab, M. Zahid, and Y. Amin, "Dual-band UWB monopole antenna for IoT applications," *Engineering Proceedings*, Vol. 46, No. 1, 29, 2023.

[11] Saleh, S., M. H. Jamaluddin, F. Razzaz, S. M. Saeed, N. Timmons, and J. Morrison, "Compactness and performance enhancement techniques of ultra-wideband tapered slot antenna: A comprehensive review," *Alexandria Engineering Journal*, Vol. 74, 195–229, 2023.

[12] Sediq, H. T., "Miniaturized MIMO antenna design based on octagonal-shaped SRR metamaterial for UWB applications," *AEU — International Journal of Electronics and Communications*, Vol. 172, 154946, 2023.

[13] Samadianfard, R., J. Nourinia, C. Ghobadi, M. Shokri, and R. Samadianfard, "A compact, ultra-thin UWB microstrip antenna for microwave imaging applications," *Soft Computing*, Vol. 27, No. 24, 19 113–19 124, 2023.

[14] Shokri, M., V. Rafii, S. Karamzadeh, Z. Amiri, and B. Virdee, "CPW-fed printed UWB antenna with open-loop inverted triangular-shaped slot for WLAN band filtering," *International Journal of Microwave and Wireless Technologies*, Vol. 8, No. 2, 257–262, 2016.

[15] Srinivasu, G., T. Gayatri, M. K. Meshram, and V. K. Sharma, "Design analysis of an ultra-wideband antenna for RF energy harvesting in 1.71–12 GHz," in *2020 11th International Conference on Computing, Communication and Networking Technologies (ICCCNT)*, 1–6, Kharagpur, India, 2020.

[16] Srinivasu, G., N. Anveshkumar, and V. K. Sharma, "A planar circular monopole UWB antenna for RF energy harvesting applications," in *2020 IEEE-HYDCON*, Hyderabad, India, 2020.

[17] Gayatri, T., G. Srinivasu, D. M. K. Chaitanya, and V. K. Sharma, "A compact Luna shaped high gain UWB antenna in 3.1 GHz to 10.6 GHz using FR4 material substrate," *Materials Today: Proceedings*, Vol. 49, 359–365, 2022.

[18] Bouchekhlal, A., A. Abed, S. E. Sahli, A. Amrouche, and R. Bendoumia, "Design of low profile, high bandwidth circular patch antenna at 28 GHz for fifth generation wireless technology," in *2023 2nd International Conference on Electronics, Energy and Measurement (IC2EM)*, Vol. 1, 1–6, 2023.

[19] Taha, B. and T. AlSharabati, "Performance comparison between the FR4 substrate and the Rogers Kappa-438 substrate for microstrip patch antennas," *International Journal of Computer Science and Mobile Computing*, Vol. 9, No. 2, 1–12, 2020.

[20] Li, W., L. Wu, S. Li, X. Cao, and B. Yang, "Bandwidth enhancement and isolation improvement in compact UWB-MIMO antenna assisted by characteristic mode analysis," *IEEE Access*, Vol. 12, 17 152–17 163, 2024.

[21] Mohammad, S. A. W., M. M. Khaleeq, T. Ali, and R. C. Biradar, "A miniaturized truncated ground plane concentric ring shaped UWB antenna for wireless applications," in *2017 2nd IEEE International Conference on Recent Trends in Electronics, Information & Communication Technology (RTEICT)*, 116–120, Bangalore, India, 2017.

[22] Kumar, S. B., A. Gandhar, M. Tiwari, A. Rehalia, and S. Gandhar, "A topical design of circularly polarized fractal boundary

antenna for RF harvesting," *Journal of Information and Optimization Sciences*, Vol. 43, No. 1, 115–121, 2022.

[23] Surender, D., M. A. Halimi, T. Khan, F. A. Talukdar, and Y. M. M. Antar, "Circularly polarized DR-rectenna for 5G and Wi-Fi bands RF energy harvesting in smart city applications," *IETE Technical Review*, Vol. 39, No. 4, 880–893, 2022.

[24] Sun, H., Y.-X. Guo, M. He, and Z. Zhong, "Design of a high-efficiency 2.45-GHz rectenna for low-input-power energy harvesting," *IEEE Antennas and Wireless Propagation Letters*, Vol. 11, 929–932, 2012.

[25] Nie, M.-J., X.-X. Yang, G.-N. Tan, and B. Han, "A compact 2.45-GHz broadband rectenna using grounded coplanar waveguide," *IEEE Antennas and Wireless Propagation Letters*, Vol. 14, 986–989, 2015.

[26] Rezazadeh, N. and L. Shafai, "A pattern diversity antenna for ambient RF energy harvesting in multipath environments," in *2018 18th International Symposium on Antenna Technology and Applied Electromagnetics (ANTEM)*, 1–4, Waterloo, ON, Canada, 2018.

[27] Wang, M., L. Yang, and Y. Shi, "A dual-port microstrip rectenna for wireless energy harvest at LTE band," *AEU — Intern. J. of Electronics and Communications*, Vol. 126, 153451, 2020.

[28] Shen, S., Y. Zhang, C.-Y. Chiu, and R. Murch, "Directional multiport ambient RF energy-harvesting system for the Internet of Things," *IEEE Internet of Things Journal*, Vol. 8, No. 7, 5850–5865, 2021.

[29] Shen, S., C.-Y. Chiu, and R. D. Murch, "Multiport pixel rectenna for ambient RF energy harvesting," *IEEE Transactions on Antennas and Propagation*, Vol. 66, No. 2, 644–656, 2018.

[30] Shen, S., C.-Y. Chiu, and R. D. Murch, "A dual-port triple-band L-probe microstrip patch rectenna for ambient RF energy harvesting," *IEEE Antennas and Wireless Propagation Letters*, Vol. 16, 3071–3074, 2017.

[31] Shen, S., Y. Zhang, C.-Y. Chiu, and R. Murch, "A triple-band high-gain multibeam ambient RF energy harvesting system utilizing hybrid combining," *IEEE Transactions on Industrial Electronics*, Vol. 67, No. 11, 9215–9226, 2019.

[32] Sharma, P., R. N. Tiwari, P. Singh, P. Kumar, and B. K. Kanaujia, "MIMO antennas: Design approaches, techniques and applications," *Sensors*, Vol. 22, No. 20, 7813, 2022.

[33] Bujjibabu, N. and S. Varadarajan, "High isolated Psi-shaped 4×4 MIMO UWB antenna for RF energy harvesting applications," *Materials Today: Proceedings*, 2023.

[34] Sharma, R., R. Khanna, and G. Kapur, "Design of metamaterial loaded wideband sub-6 GHz 2×1 MIMO antenna with enhanced isolation using characteristic mode analysis," *Wireless Personal Communications*, Vol. 134, No. 3, 1713–1736, 2024.

[35] Sakli, H., C. Abdelhamid, C. Essid, and N. Sakli, "Metamaterial-based antenna performance enhancement for MIMO system applications," *IEEE Access*, Vol. 9, 38 546–38 556, 2021.

[36] Garg, P. and P. Jain, "Isolation improvement of MIMO antenna using a novel flower shaped metamaterial absorber at 5.5 GHz WiMAX band," *IEEE Transactions on Circuits and Systems II: Express Briefs*, Vol. 67, No. 4, 675–679, 2020.

[37] Chouhan, S., D. K. Panda, V. S. Kushwah, and P. K. Mishra, "Octagonal-shaped wideband MIMO antenna for human interface device and S-band application," *Intern. J. of Microwave and Wireless Technologies*, Vol. 11, No. 3, 287–296, 2019.

[38] Rajeshkumar, V. and R. Rajkumar, "SRR loaded compact tri-band MIMO antenna for WLAN/WiMAX applications," *Progress In Electromagnetics Research Letters*, Vol. 95, 43–53, 2020.

[39] Yang, C., J. Kim, H. Kim, J. Wee, B. Kim, and C. Jung, "Quad-band antenna with high isolation MIMO and broadband SCS for broadcasting and telecommunication services," *IEEE Antennas and Wireless Propagation Letters*, Vol. 9, 584–587, 2010.

[40] Bhattacharya, A. and B. Roy, "Investigations on an extremely compact MIMO antenna with enhanced isolation and bandwidth," *Microwave and Optical Technology Letters*, Vol. 62, No. 2, 845–851, 2020.

[41] Kumar, A., N. K. Narayaswamy, H. V. Kumar, B. Mishra, S. A. Siddique, and A. K. Dwivedi, "High-isolated WiFi-2.4 GHz/LTE MIMO antenna for RF-energy harvesting applications," *AEU — International Journal of Electronics and Communications*, Vol. 141, 153964, 2021.

[42] Luo, S., D. Wang, Y. Chen, E. Li, and C. Jiang, "A compact dual-port UWB-MIMO antenna with quadruple band-notched characteristics," *AEU — International Journal of Electronics and Communications*, Vol. 136, 153770, 2021.

[43] Xiong, K., A. Nallanathan, and C. Wang, "Energy efficient MIMO-based cooperative communications for wireless networks: A distributed approach," *IEEE Transactions on Communications*, Vol. 65, No. 1, 151–164, 2017.

[44] Li, S., Z. Wan, L. Jin, and J. Du, "Energy harvesting maximizing for millimeter-wave massive MIMO-NOMA," *Electronics*, Vol. 9, No. 1, 32, 2019.

[45] Roy, S., R. J.-J. Tiang, M. B. Roslee, M. T. Ahmed, and M. A. P. Mahmud, "Quad-band multiport rectenna for RF energy harvesting in ambient environment," *IEEE Access*, Vol. 9, 77 464–77 481, 2021.

[46] Uwiringiyimana, J. P., U. Khayam, Suwarno, and G. C. Montanari, "Design and implementation of ultra-wide band antenna for partial discharge detection in high voltage power equipment," *IEEE Access*, Vol. 10, 10 983–10 994, 2022.

[47] Parameswari, S. and C. Chitra, "Compact textile UWB antenna with hexagonal for biomedical communication," *Journal of Ambient Intelligence and Humanized Computing*, 1–8, 2021.

[48] Fakharian, M. M., "A wideband rectenna using high gain fractal planar monopole antenna array for RF energy scavenging," *International Journal of Antennas and Propagation*, Vol. 2020, No. 1, 3489323, 2020.

[49] Piñuela, M., P. D. Mitcheson, and S. Lucyszyn, "Ambient RF energy harvesting in urban and semi-urban environments," *IEEE Transactions on Microwave Theory and Techniques*, Vol. 61, No. 7, 2715–2726, 2013.

[50] Vuong, T.-P., D. H. N. Bui, J. Verdier, B. Allard, and P. Benech, "Design and measurement of 3D flexible antenna diversity for ambient RF energy scavenging in indoor scenarios," *IEEE Access*, Vol. 7, 17 033–17 044, 2019.

[51] Jabire, A. H., S. Sani, S. Saminu, M. J. Adamu, and M. I. Hussein, "A crossed-polarized four port MIMO antenna for UWB communication," *Heliyon*, Vol. 9, No. 1, 2023.

[52] Savcı, H. S., "A four element stringray-shaped MIMO antenna system for UWB applications," *Micromachines*, Vol. 14, No. 10, 1944, 2023.

[53] Malekpour, N. and M. A. Honarvar, "Design of high-isolation compact MIMO antenna for UWB application," *Progress In Electromagnetics Research C*, Vol. 62, 119–129, 2016.

[54] Abdelghany, M. A., M. F. A. Sree, A. Desai, and A. A. Ibrahim, "4-port octagonal shaped MIMO antenna with low mutual coupling for UWB applications," *Computer Modeling in Engineering & Sciences (CMES)*, Vol. 136, No. 2, 1999–2015, 2023.